Topographic Organization of the Basal Forebrain Projections to the Perirhinal, Postrhinal, and Entorhinal Cortex in Rats

Hideki Kondo and Laszlo Zaborszky*

Center for Molecular and Behavioral Neuroscience, Rutgers, The State University of New Jersey, Newark, New Jersey 07102

ABSTRACT

Previous studies have shown that the basal forebrain (BF) modulates cortical activation via its projections to the entire cortical mantle. However, the organization of these projections is only partially understood or, for certain areas, unknown. In this study, we examined the topographic organization of cholinergic and noncholinergic projections from the BF to the perirhinal, postrhinal, and entorhinal cortex by using retrograde tracing combined with choline acetyltransferase (ChAT) immunohistochemistry in rats. The perirhinal and postrhinal cortex receives major cholinergic and noncholinergic input from the caudal BF, including the caudal globus pallidus and substantia innominata and moderate input from the horizontal limb of the diagonal band, whereas the entorhinal cortex receives major input from the rostral BF, including the medial septum and the vertical and horizontal limbs of the diagonal band. In the perirhinal cases, cholinergic projection neurons are distributed more caudally in the caudal globus pallidus than noncholinergic projection neurons. Compared with the perirhinal cases, the distribution of cholinergic and noncholinergic neurons projecting to the postrhinal cortex shifts slightly caudally in the caudal globus pallidus. The distribution of cholinergic and noncholinergic neurons projecting to the lateral entorhinal cortex extends more caudally in the BF than to the medial entorhinal cortex. The ratio of ChAT-positive projection neurons to total projection neurons is higher in the perirhinal/postrhinal cases (26–48%) than in the entorhinal cases (13–30%). These results indicate that the organization of cholinergic and noncholinergic projections from the BF to the parahippocampal cortex is more complex than previously described. J. Comp. Neurol. 524:2503–2515, 2016.

INDEXING TERMS: cholinergic and noncholinergic neurons; parahippocampal region; medial septum; vertical and horizontal limbs of diagonal band; substantia innominata; globus pallidus; retrograde tracing

The basal forebrain (BF) is composed of heterogeneous structures, including the medial septum (MS), vertical and horizontal limbs of the diagonal band (VDB, HDB), substantia innominata (SI), and globus pallidus (GP), and provides topographically organized cholinergic projections to the entire cortical mantle (Bigl et al., 1982; Lamour et al., 1982; McKinney et al., 1983; Mesulam et al., 1983a,b; Price and Stern, 1983; Rye et al., 1984; Saper, 1984; Woolf et al., 1984; Amaral and Kurz et al., 1985; Luiten et al., 1987; Gaykema et al., 1990; Ghashghaei and Barbas, 2001; Bloem et al., 2014; Zaborszky et al., 2015a). Additionally, the BF sends noncholinergic projections, including γ-aminobutyric acid (GABA)ergic, glutamatergic, and peptidergic axons to the cortex (Gritti et al., 1997; Hur and Zaborszky, 2005; Zaborszky et al., 2015b). It has been shown that the BF projection, including cholinergic projection, to the cortex plays a critical role in cortical activation and is also implicated in attention, sensory processing, and learning (Buzsaki et al., 1988; Metherate et al., 1992; Muir et al., 1993; Everitt and Robbins, 1997; Dringenberg and Vanderwolf, 1998; Detari et al., 1999; Duque et al., 2000: Jones, 2004; Lin and Nicolelis, 2008; Fuller et al., 2011; Letzkus et al., 2011; Pinto et al., 2013).

Grant sponsor: National Institute for Neurological Disorders and Stroke, National Institutes of Health; Grant number: 23945 (to L.Z.).

*CORRESPONDENCE TO: Laszlo Zaborszky, Center for Molecular and Behavioral Neuroscience, Rutgers, The State University of New Jersey, Newark, New Jersey 07102. E-mail: laszloz@andromeda.rutgers.edu

Received January 3, 2015; Revised July 2, 2015;
Accepted January 13, 2016.
DOI 10.1002/cne.23967
Published online February 17, 2016 in Wiley Online Library (wileyonlinelibrary.com)

Despite several previous anatomical studies, a systematic study of the topographic organization of the BF projections to the perirhinal (PER), postrhinal (POR), and entorhinal cortex (EC) has not been done. The PER and POR receives convergent inputs from several sensory and nonsensory association areas and provides major cortical input to the entorhinal cortex, which in turn sends major cortical input to the hippocampus (Suzuki and Amaral, 1994; Burwell and Amaral, 1998a,b; Witter et al., 2000; Furtak et al., 2007). In the present study, we examined the topographic organization of the BF projections to the PER, POR, and EC using retrograde tracers in combination with choline acetyltransferase (ChAT) immunostaining in rats.

MATERIALS AND METHODS

Forty-one male Sprague–Dawley rats (Harlan, Indianapolis, IN; weight 167–208 g) were used in this study. Of these animals, we used 16 successful cases for further analysis after checking for proper uptake and transport of the tracer, and that injections were restricted to the target cortical region. All experiments were performed in accordance with the US Public Health Service Policy on Human Care and Use of Laboratory Animals and the National Institutes of Health Guidelines for the Care and Use of Animals in Research, and were approved by Rutgers University Institutional Review Board.

Tracer injections

Unilateral injections of the retrograde tracers Fast Blue (FB; Polysciences, Warrington, PA) and Fluoro-Gold (FG; Fluorochrome, Denver, CO), both 2% solution in purified water, were made in the PER, POR, and entorhinal cortex. Animals were anesthetized with isoflurane. FB was injected by pressure injection (PV820 device; World Precision Instrument, Sarasota, FL) using glass pipettes (tip diameter, 40–80 μm), and FG was iontophoretically injected by applying a negative, pulsed DC current (7 μA; 7-second on–off cycles; 20 minutes). To avoid leakage along the pipette track, we used a modified stereotaxic instrument (SR-50, Narishige, East Meadow, NY) allowing rotation of the head position of up to 90 degrees. After a survival period of 6–10 days, the animals were deeply anesthetized with isoflurane supplemented with urethane (1.5 ml of a 0.35 g/ml solution) and transcardially perfused with 0.9% saline, followed by 4% paraformaldehyde in 0.1 M phosphate buffer (PB). The brains were removed from the skull, postfixed for 4 hours in the same fixative, and stored in 30% sucrose.

Abbreviations

BF	basal forebrain
ChAT	choline acetyltransferase
EC	entorhinal cortex
FB	Fast Blue
FG	Fluoro-Gold
GP	globus pallidus
HDB	horizontal limb of the diagonal band
ic	internal capsule
LEC	lateral entorhinal cortex
MEC	medial entorhinal cortex
MS	medial septum
PER	perirhinal cortex
POR	postrhinal cortex
RS	retrosplenial cortex
SI	substantia inominata
VDB	vertical limb of the diagonal band

Tissue processing

The brains were cut on a freezing microtome in the coronal plane (50 μm thickness) and collected in 0.1 M PB. Four alternating series of sections were made; the first series of sections was mounted for FB and FG without further processing, the second series of sections was stained with Nissl, the third series was processed for ChAT immunohistochemistry, and the fourth series was stored in a cryoprotectant and stored at −20°C. Following mapping with the epifluorescent microscope, coverslips were removed and sections were restained with thionine to identify cytoarchitectonic areas. Images of the Nissl-stained sections were overlaid with the appropriate mapping files using the Neurolucida "virtual slice module."

ChAT processing was as follows. After washing (3 × 10 minutes) in 0.1 M PB, sections were incubated in goat anti-ChAT antibody (1:500, EMD Millipore, Billerica, MA; RRID: AB_2079751) (Table 1) at room temperature (RT) overnight. Sections were subsequently rinsed for 3 × 10 minutes in 0.1 M PB and incubated in Cy3 (indocarbocyanine) IgG or Cy2 (cyanine) IgG conjugated to donkey anti-goat IgG (1:200, Jackson ImmunoResearch, West Grove, PA; RRID: AB_2307351 and AB_2307341, respectively) for 3 hours at RT. Sections were then rinsed for 3 × 10 minutes in 0.1 M PB. The same primary and linking antibodies were used in two previous publications from this laboratory (Unal et al., 2012, 2015).

Sections were mounted on glass slides and, after drying at RT, were coverslipped with DEPEX mounting medium (Electron Microscopy Sciences, Hatfield, PA). To better localize the projection neurons, sections after plotting were counterstained with Nissl.

Method of analysis

The location and extent of each injection and the distribution of retrogradely (cholinergic and noncholinergic) labeled cells in the BF were plotted from the histological sections with a Zeiss Axioscop microscope equipped with a Neurolucida (MBF Bioscience, Williston, VT;

TABLE 1.
Antibodies Used in This Study

Antigen	Immunogen	Source	Dilution
Anti-ChAT	Human placental enzyme	EMD Millipore Goat polyclonal, cat# AB144P, RRID: AB_2079751	1:500
Cy2 anti-goat		Jackson ImmunoResearch Donkey polyclonalcat# 705-225-147 RRID: AB_2307341	1:200
Cy3 anti-goat		Jackson ImmunoResearch Donkey polyclonalcat# 705-165-147 RRID: AB_2307351	1:200

RRID: nif-0000-10294) software and hardware data acquisition system. By using the Zeiss epifluorescent microscope with the appropriate filter set (UV G365/LP420; Blue BP450/490-LP520; Green BP546/12-LP590 AXIO), the FB- and FG-labeled projection neurons and the CY3-labeled cholinergic neurons could be separately visualized in the same section. Cytoarchitectonically defined borders of BF regions were added to the maps, guided by Nissl staining of the mapped sections. For quantitative analysis, the numbers of ChAT-negative and ChAT-positive projection neurons in the BF were counted using MBF Explorer, and the ratio of ChAT-positive and -negative projection cells to the total projection cells was then calculated. To compare the location and number of retrogradely labeled cells in the septum and caudal GP in the individual cases, the mapped series of sections that were 200 μm apart was reorganized and normalized so each section became equidistant to the same fiducial markers. Statistics were done using one-way analysis of variance (ANOVA) with Tukey's post hoc test. The graphical data in Figure 10 represent the mean and standard error of the mean obtained by using Excel.

Injection sites were defined based on the extent of dense fluorescent labeling with the surrounding halo and the relationship to cytoarchitectonically defined cortical areas in Nissl-stained sections according to Burwell (2001). In this text, for BF areas we tried to adhere to the nomenclature adapted by Paxinos and Watson (2005), except for the magnocellular preoptic nucleus, which we incorporated into the area of the horizontal limb of the diagonal band (HDB), and we kept the term substantia innominata (SI) for the "extended amygdala," as replacing the classical term would diminish the significance of the corticopetal system (see detailed discussion in Zaborszky et al., 2015c).

RESULTS

BF projections to the perirhinal cortex

In total, seven injections (FB and FG) were made at various rostrocaudal levels of the perirhinal cortex (Table 2). Retrogradely labeled cells were found in each subregion of the BF; dense labeling was present in the caudal BF, including caudal GP and SI. Labeling was weak in the rostral BF (MS/VDB). Double-labeled cells (ChAT-positive and retrogradely labeled cells) were densely packed in the caudal GP but were also observed in other BF regions.

Three injections (FB and FG) were made in the rostral PER (Table 2, Fig. 8A). In a representative case (case R-25), FG was injected in area 36 of the rostral PER (Fig. 1). Retrogradely labeled cells were observed most densely in the caudal GP (Fig. 1E–G), moderately in the HDB and caudal SI (Fig. 1C–G), and sparsely in the MS/VDB (Fig. 1A). ChAT-positive and ChAT-negative projection neurons were distributed in each subregion of the BF. Generally, in the GP, between 1.6 and 2.4 mm caudal to bregma there are more noncholinergic projection neurons than cholinergic neurons (Fig. 10). However, caudally, between 2.6 and 2.8 mm there are more cholinergic projection than noncholinergic neurons (Fig. 10). In the entire BF from three cases, 48% of labeled projection neurons were ChAT positive (n = 382; Table 3).

TABLE 2.
Retrograde Tracer Injections in ihe Perirhinal, Postrhinal, and Entorhinal Cortex[1]

Area injected	Case no.	Tracer	Layers
Perirhinal cortex			
(Rostral)			
Area 35	R-21	FG	I, II, III
Area 36	R-25	FG	II, III, IV, V
Area 36	R-41	FB	I, II, III, IV, V, VI
(Middle)			
Area 36	R-33	FG	I, II, III, IV, V
Area 36	R-39	FB	I, II, III, IV, V
Area 36	R-47	FB	I, II, III
(Caudal)			
Area 36	R-51	FB	I, II, III, IV, V
Postrhinal cortex			
POR (m-c)	R-29	FB	I, II, III
POR (m-c)	R-49	FB	I, II, III
Entorhinal cortex			
LEC (L)	R-27	FG	III, V
LEC (I)	R-28	FB	I, II
LEC (L)	R-28	FG	V, VI
LEC (L)	R-44	FG	V, VI
MEC (L)	R-14	FG	II, III, V
MEC (M)	R-41	FG	III, V
MEC (I)	R-49	FG	V, VI

[1]L, I, M, and m-c in parentheses indicate the lateral, intermediate, and medial part of the entorhinal injections and the mid-caudal part of the postrhinal cortex. For other abbreviations, see list.

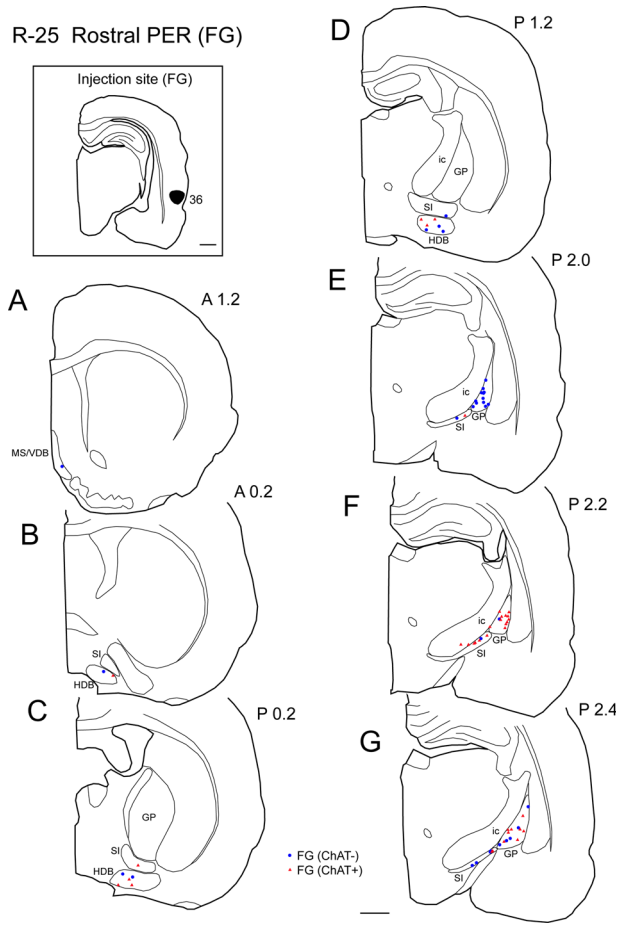

Figure 1. A–G: Distribution of retrogradely labeled cells in the basal forebrain (BF) following an injection of FG into the rostral perirhinal cortex (PER; area 36; case R-25 FG). A black-filled area on the boxed coronal section shows the location of the FG injection site (top left). Line drawings were arranged from rostral to caudal (A–G). Retrogradely labeled cells positive for ChAT are shown by red triangle (ChAT+); noncholinergic retrogradely labeled cells are indicated by blue filled circle (ChAT−). Note that labeling is denser in the caudal part of the BF, including the caudal globus pallidus (GP) and substantia innominata (SI). Within the caudal GP, it is apparent that noncholinergic projection neurons outnumber cholinergic projection cells rostrally (E), whereas cholinergic cells are more numerous caudally (F–G). Scale bar = 1 mm in G (applies to A–G).

Three injections (FB and FG) were made in the mid-perirhinal cortex (Table 2). In a representative case (case R-47; Fig. 2), FB was injected in area 36 at the mid-rostrocaudal level of the PER. Retrogradely labeled cells were observed most densely in the caudal GP/SI (Fig. 2F,G), and labeling decreased rostrally. Similar to case R-25, ChAT-positive projection neurons were present most densely in the caudal GP (Fig. 2G). In the GP, between approximately 1.6 and 2.6 mm there were more noncholinergic projection neurons than cholinergic ones, but this difference leveled off at about 2.8 mm caudal to bregma (Fig. 10). In the entire BF, from three animals, 38% of labeled projection neurons were ChAT positive (n = 608; Table 3).

One injection was made in the caudal PER (Table 2, Fig. 8B). In case R-51, FB was injected in area 36 at the caudal level of the perirhinal cortex. As in the rostral and mid-perirhinal cases, labeled cells were found most densely in the caudal part of the GP and SI (Figs. 3F,G, 9B) and were present very sparsely in the rostral BF (Figs. 3A–C, 9A). Similar to rostral and mid-perirhinal injections, noncholinergic cells between 2.2 and 2.8 mm were more numerous than cholinergic projection neurons (Fig. 10). In the entire BF, only 26% of

TABLE 3.

Number of cholinergic and Noncholinergic Neurons in the Basal Forebrain Projecting to the Perirhinal, Postrhinal, and Entorhinal Cortex[1]

Case		MS/VDB	HDB	SI	SI (c)	GP	Total	%
Perirhinal cortex								
(Rostral)								
R-21 FG	ChAT−	0	8	11	31	50	100	52
	ChAT+	3	25	9	21	35	93	48
R-25 FG	ChAT−	3	7	5	7	28	50	52
	ChAT+	0	10	4	8	25	47	48
R-41 FB	ChAT−	1	22	10	7	12	52	57
	ChAT+	1	4	8	6	21	40	43
(mid)								
R-33 FG	ChAT−	4	21	9	28	89	151	60
	ChAT+	5	13	4	23	54	99	40
R-39 FB	ChAT−	2	3	9	33	54	101	60
	ChAT+	3	15	2	19	27	66	40
R-47 FB	ChAT−	3	7	6	30	80	126	66
	ChAT+	3	15	3	14	30	65	34
(Caudal)								
R-51 FB	ChAT−	2	6	5	66	68	147	74
	ChAT+	4	7	2	12	28	53	26
Postrhinal cortex								
R-29 FB	ChAT−	8	6	8	24	27	73	54
	ChAT+	1	1	0	19	40	61	46
R-49 FB	ChAT−	11	4	4	63	18	100	60
	ChAT+	13	6	2	22	25	68	40
Entorhinal cortex								
LEC								
R-27 FG	ChAT−	301	134	22	4	4	465	77
	ChAT+	59	67	9	3	0	138	23
R-28 FB	ChAT−	295	93	18	2	5	413	77
	ChAT+	91	28	1	0	0	120	23
R-28 FG	ChAT−	471	107	11	1	4	594	87
	ChAT+	49	33	4	0	1	87	13
R-44 FG	ChAT−	152	19	3	0	2	176	79
	ChAT+	14	30	3	0	0	47	21
MEC								
R-14 FG	ChAT−	172	16	0	1	0	189	70
	ChAT+	61	21	0	0	0	82	30
R-41 FG	ChAT−	117	9	1	0	0	127	77
	ChAT+	27	11	0	0	0	38	23
R-49 FG	ChAT−	276	51	0	1	0	328	82
	ChAT+	50	22	0	0	0	72	18

[1] For abbreviations, see list. % of the number of ChAT+ or ChAT− to the total retrograde cells. SI(c) caudal part of SI.

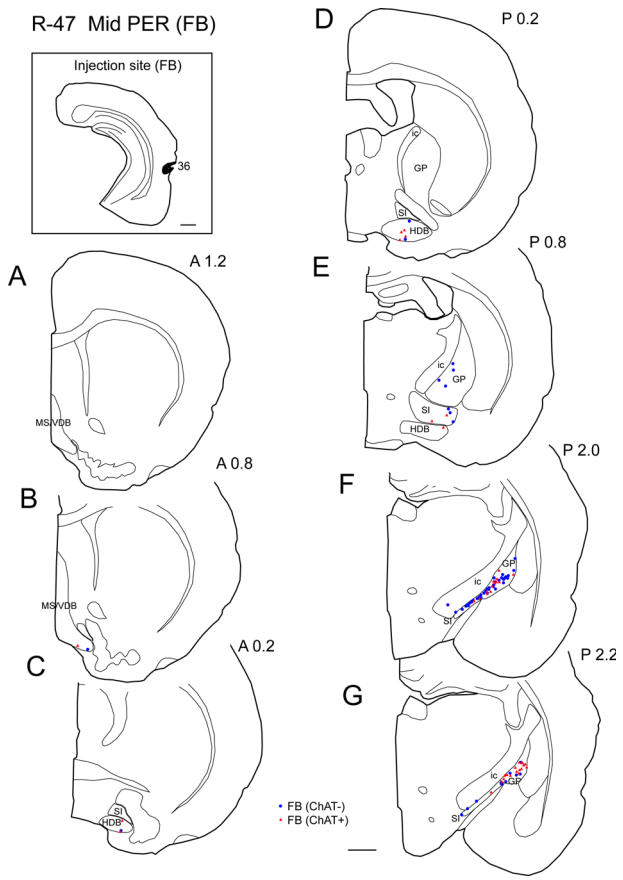

Figure 2. **A–G:** Distribution of cholinergic and noncholinergic retrogradely labeled cells following an injection of FB into the mid-rostrocaudal portion of the perirhinal cortex (case R-47 FB). Conventions as in Figure 1. Note that, as in Figure 1, labeling is present most densely in the caudal basal forebrain (caudal GP and SI; F,G) and decreases rostrally. Cholinergic projection neurons are present densely in the caudal part of the caudal GP (G). For abbreviations, see list. Scale bar = 1 mm in G (applies to A–G).

labeled projection neurons were ChAT positive (n = 200; Table 3). In comparison with the rostral and mid-rostrocaudal PER cases, the ratio of cholinergic projection neurons was lower in the caudal perirhinal cortex (Table 3).

BF projections to the postrhinal cortex

In total, two injections (FB) were made in the postrhinal cortex. As in the perirhinal cases, retrogradely labeled cells were found densely in the caudal BF (caudal GP/SI), with density decreasing rostrally.

In the representative case (case R-29), FB was injected in the mid-caudal POR (Fig. 8C), and labeled cells were present most densely in the caudal GP/SI (Figs. 4E–G, 9C) and sparsely in the HDB, VDB, and SI (Fig. 4A–D). Cholinergic projection neurons were intermingled with noncholinergic projection neurons and were found most densely in the caudal GP/SI. Within the caudal GP/SI, the density of cholinergic neurons was higher in the caudal than in the rostral part (Fig. 4E–G). Compared with the perirhinal cases, the distribution of cholinergic and noncholinergic projection neurons shifted slightly caudally in the caudal GP (Fig. 10). In the entire BF, from two animals, 43% of labeled projection neurons were ChAT positive (n = 302; Table 3).

BF projections to the entorhinal (EC) cortex

Four injections (FG and FB) in the lateral EC (LEC) and three injections (FG) in medial EC (MEC) were made. Unlike in the perirhinal and postrhinal cases, retrogradely labeled cells were densely present in the rostral BF (MS/VDB) (Figs. (5 and 6), 9D) and were absent or very few in the caudal BF. The ratio of noncholinergic

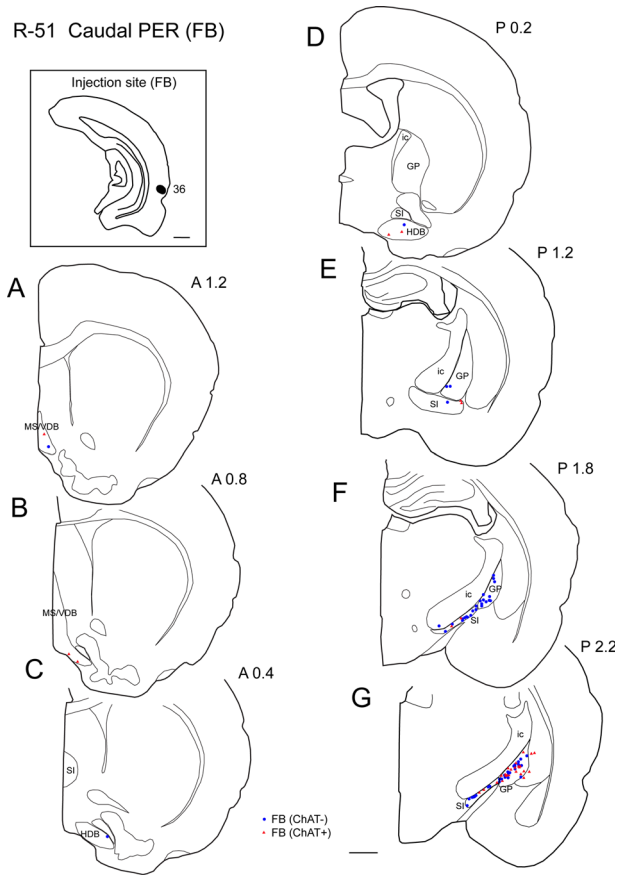

Figure 3. **A–G:** Distribution of cholinergic and noncholinergic retrogradely labeled cells following an injection of FB into the caudal portion of the perirhinal cortex (case R-51 FB). Conventions as in Figure 1. Note that, as in Figures 1 and 2, labeling is present densely in the caudal basal forebrain (caudal GP and SI; F,G) and decreases rostrally. Cholinergic projection neurons are present densely in the caudal part of the caudal GP (G). For abbreviations, see list. Scale bar = 1 mm in G (applies to A–G).

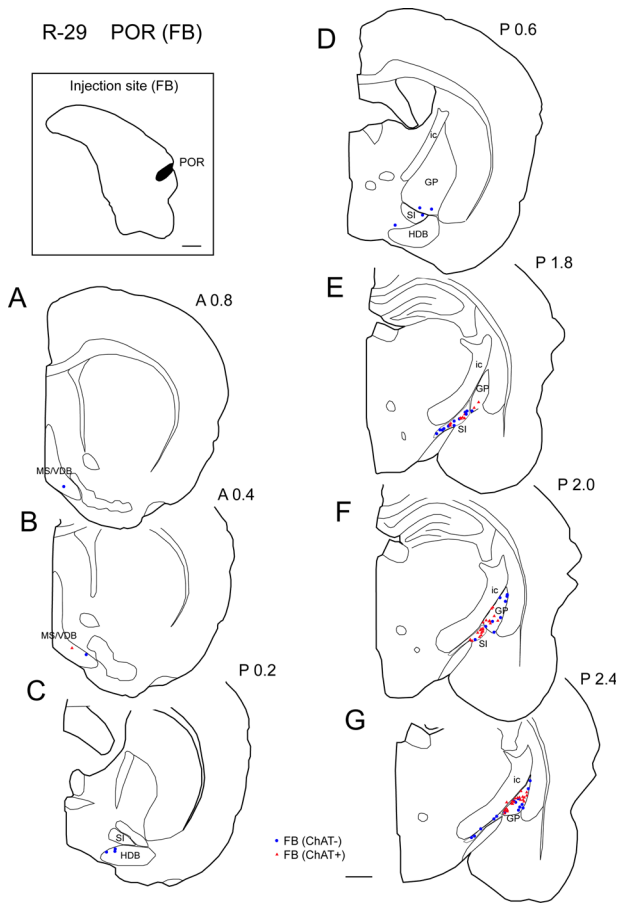

Figure 4. **A–G:** Distribution of cholinergic and noncholinergic retrogradely labeled cells following an injection of FB into the postrhinal cortex (case R-29 FB). Conventions as in Figure 1. Note that, as in perirhinal cases (Figs. 1–3), labeling is dense in the caudal basal forebrain (caudal GP and SI; E–G) and decreases rostrally (A–D). Cholinergic projection neurons are labeled densely in the caudal part of the caudal GP (F,G). For abbreviations, see list. Scale bar = 1 mm in G (applies to A–G).

to cholinergic projection neurons in EC cases (3.9) was higher than that in the perirhinal (1.5) and postrhinal (1.3) cases.

In the representative case of LEC injection (case R-27), FG was injected in the dorsolateral part of the LEC, and labeled cells were observed very densely in the MS/VDB (Fig. 5A,B), extending to the HDB and SI (Fig. 5C–F). In the caudal MS/VDB, cholinergic projection neurons were found more densely in the ventral than in the dorsal part (Fig. 5B). In the entire BF, from four cases only 19% of labeled projection neurons were colocalized with ChAT (n = 2,040; Table 3).

In the representative case of MEC injection (case R-49 FG), FG was injected in the caudal MEC (Fig. 6). As in case R-27, labeled cells were densely present in the MS/VDB (Fig. 6A,B). Labeling in LEC cases extended more caudally (1.8–2.2 mm) than in cases with MEC injections (1.2 mm; Fig. 10); of three cases, 23% of labeled projection neurons were ChAT positive (n = 836; Table 3).

Figure 7 shows the topographical specificity of the HDB projections to the perirhinal and entorhinal cortex, as this BF subdivision contains cells projecting to all cortical areas investigated in this study. In the case of MEC (Fig. 7B), cells were located medially, whereas they were present more diffusely in the case of LEC (Fig. 7A). Finally, labeling in the HDB in MEC cases seemed to be different from the pattern of labeling in a perirhinal case, where labeled cells occupied the midportion of the HDB (Fig. 7C).

Comparison of the total number of projection (cholinergic + noncholinergic) neurons normalized for the size of injection surface (10^6 μm^2) limited to cases in which FG was injected in the PER (n = 3), MEC (n = 3), and LEC (n = 3) showed a trend toward an increasing

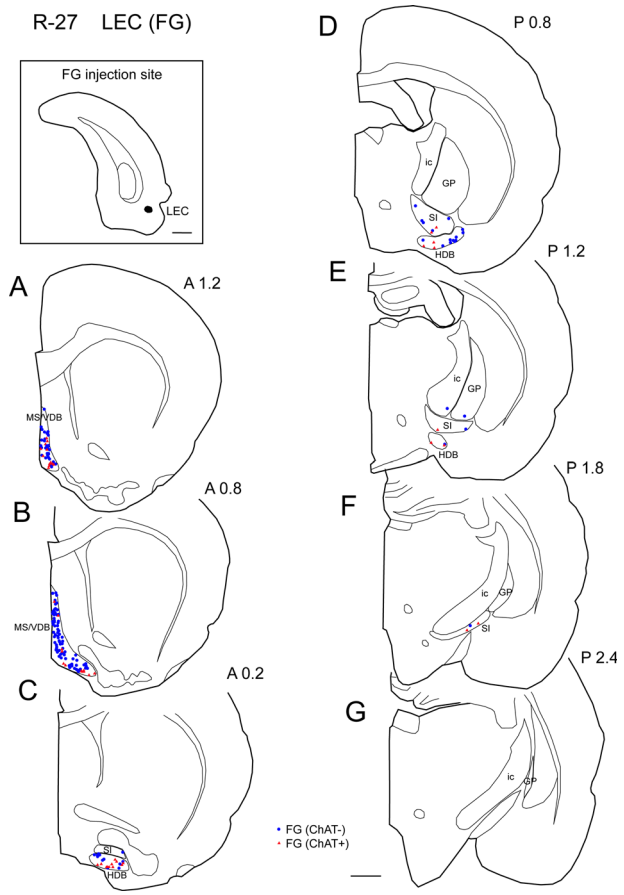

Figure 5. **A–G:** Distribution of cholinergic and noncholinergic retrogradely labeled cells following an injection of FG into the lateral entorhinal cortex (LEC; case R-27 FG). Conventions as in Figure 1. Note that in contrast to the topographic pattern of labeling in the perirhinal and postrhinal cases (Figs. 1–4), labeling is present densely in the rostral BF (MS/VDB) (A,B). For abbreviations, see list. Scale bar = 1 mm in G (applies to A–G).

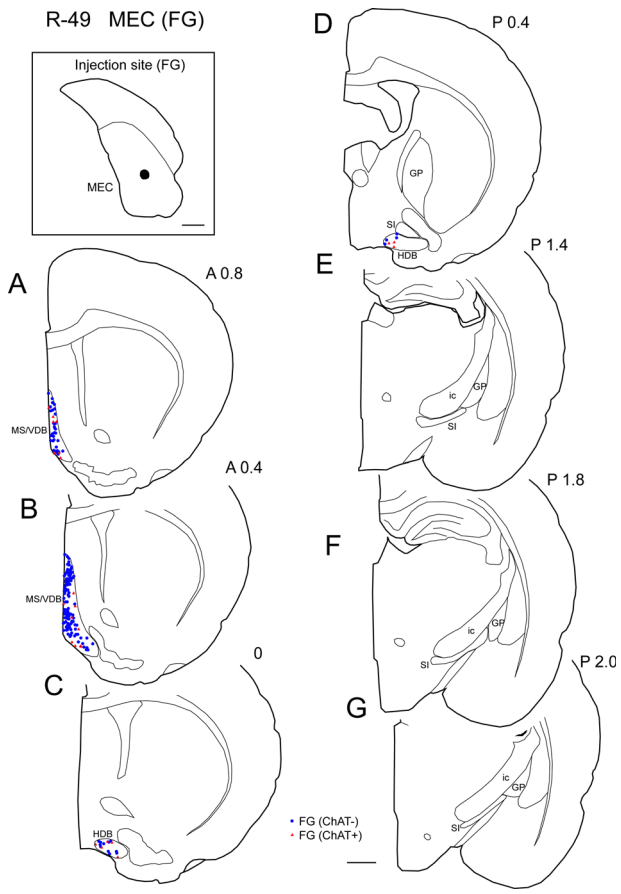

Figure 6. **A–G:** Distribution of cholinergic and noncholinergic retrogradely labeled cells following an injection of FG into the medial entorhinal cortex (case R-49 FG). Conventions as in Figure 1. Note that as in the LEC case (Fig. 5), labeling is present densely in the rostral BF (MS/VDB) (A,B). Compared with the LEC case (Fig. 5), labeling is confined to more rostral regions in the BF. For abbreviations, see list. Scale bar = 1 mm in G (applies to A–G).

number of total projection neurons from the PER (45.4 ± 9.2) to the LEC (203.2 ± 43.4), with values of the MEC (131.3 ± 40.5) in between; the difference between the PER and LEC was significant ($P < 0.5$).

DISCUSSION

In the present study, we examined the topographic organization of the BF projections to the perirhinal, postrhinal, and entorhinal cortex. We found that these cortical areas receive complementary inputs from the BF in that the perirhinal and postrhinal cortex receives cholinergic and noncholinergic projections mainly from the caudal part of the BF, including the GP/SI, as well as from the HDB, whereas the entorhinal cortex (LEC and MEC) receives cholinergic and noncholinergic projections mainly from the rostral part of the BF (MS/VDB) as well as from the HDB (Fig. 11). The overall number of retrogradely labeled cells projecting to the EC is much higher than to the PER. The ratio of cholinergic projection neurons to total projection neurons is higher in PER/POR cases (26-48%) than in EC cases (13–30%). We also revealed that in comparison with PER cases, the distribution of cholinergic and noncholinergic GP neurons projecting to the POR shifts slightly caudally within the caudal GP. Furthermore, the distribution of cholinergic and noncholinergic neurons projecting to the LEC extends more caudally in the BF than to the MEC. A differential distribution of BF projection neurons according to their cholinergic and/or noncholinergic transmitter (GP: Fig. 10) or their target (HDB: Fig. 7) suggests an organization that is more specific

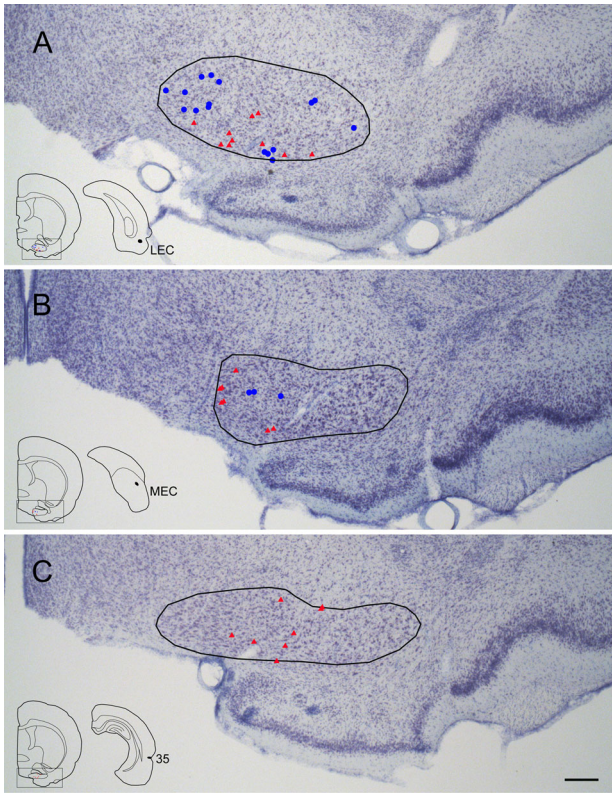

Figure 7. **A–C:** Distribution of retrogradely labeled cells in the HDB following FG injections in the LEC (A, case R-27 FG), MEC (B, case R-14 FG), and perirhinal cortex (C, case R-21 FG). Labeled cells are superimposed on the Nissl-stained images of the mapped sections. Blue circles and red rectangles indicate noncholinergic and cholinergic retrogradely labeled cells, respectively. The injection site and the actual mapped coronal section are shown in the lower left inset. The boxed area on the coronal map shows the position of the picture, and the outline on the Nissl section shows the border of the HDB. Note that the labeled cells are located medially in the HDB in the case of the MEC injection (B), whereas labeling is present in both medial and ventral portions of the HDB in the case of the LEC injection (A). In the perirhinal case, labeling is shifted to the midportion of HDB (C). For abbreviations, see list. Scale bar = 0.25 mm in C (applies to A–C).

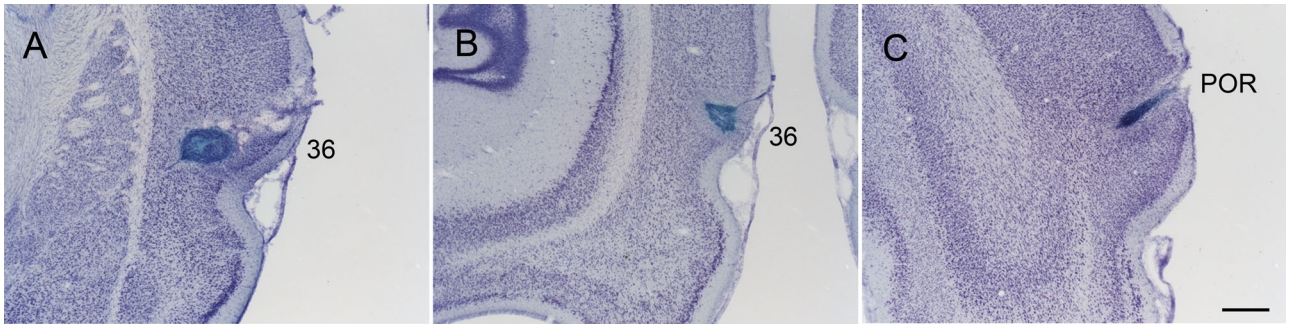

Figure 8. **A–C:** Photomicrographs showing representative injection sites of Fast Blue in the rostral perirhinal cortex (A, R-41), caudal perirhinal cortex (B, R-51), and postrhinal cortex (POR; C, R-29) on Nissl sections. Scale bar = 0.5 mm in C (applies to A–C).

than previously described. The comparison of the fine topography of neurons projecting to the PER, POR, and EC with pools of BF neurons that project to other cortical targets suggests interactions within the BF that support specific cognitive operations.

Basal forebrain projections to the perirhinal, postrhinal, and entorhinal cortex

To our knowledge, the present study is the first to systematically examine the topographic organization of the cholinergic and noncholinergic projections to the perirhinal, postrhinal, and entorhinal cortex, although some previous findings are consistent with our present results. Saper (1984) found that following a horseradish peroxidase–wheat germ agglutinin (HRP-WGA) injection in the rat perirhinal cortex, retrogradely labeled cells were present in the ventrolateral part of the caudal GP. Woolf et al. (1984) reported cholinergic projections to the perirhinal cortex from the "subpallidal SI" and "nucleus basalis" in rats. However, inadequate documentation in those studies prevents a detailed comparison of the findings with the present study. In the present study, we

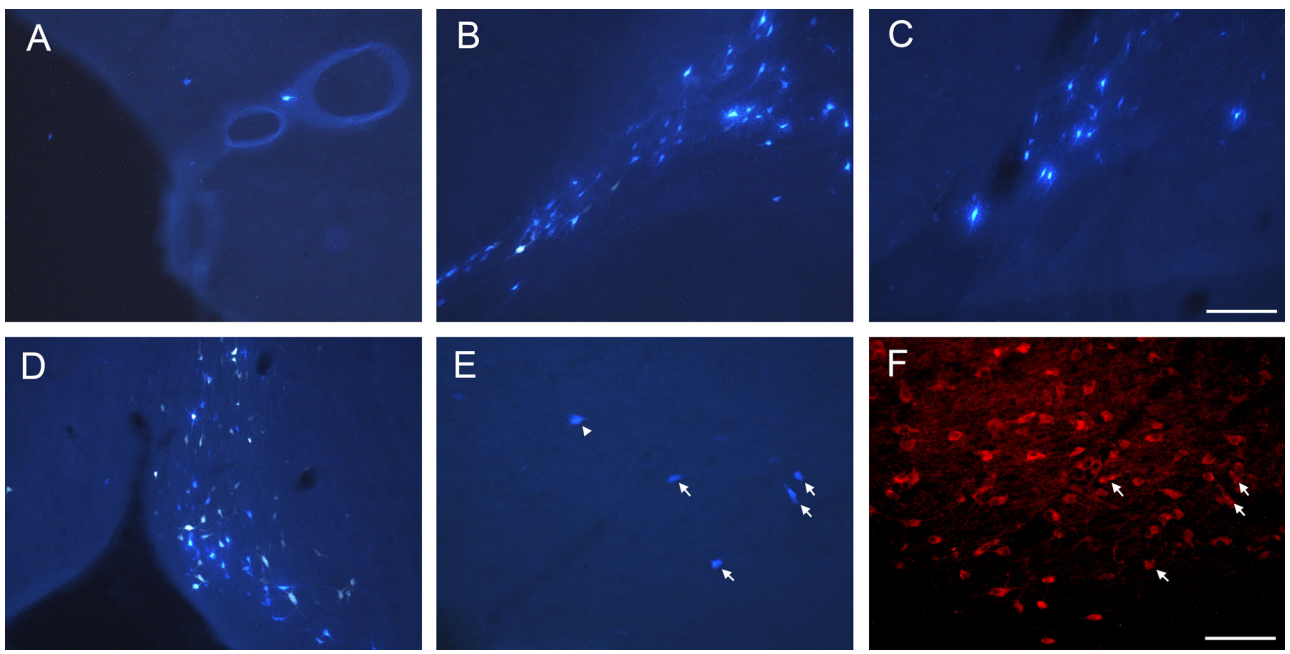

Figure 9. **A–F:** Photomicrographs of retrogradely labeled cells in the HDB (A) and caudal GP (B) following FB injection in the caudal perirhinal cortex (case R-51 FB), in the caudal GP (C) following FB injection in the postrhinal cortex (case R-29 FB), and in the MS/VDB (D) following FB injection in the entorhinal cortex (case R-28 FB). Photomicrographs in E and F show the retrogradely labeled cells in the HDB (E) following FB injection in the caudal perirhinal cortex (case R-50 FB) and immunoreactive cells for ChAT (F) for the same location as in E. Arrows indicate double-labeled cells for FB and ChAT (E,F), and an arrowhead indicates an FB-labeled cell that is ChAT negative (E). For abbreviations, see list. Scale bar = 0.1 mm in C (applies to A–D); 0.2 mm in F (applies to E,F).

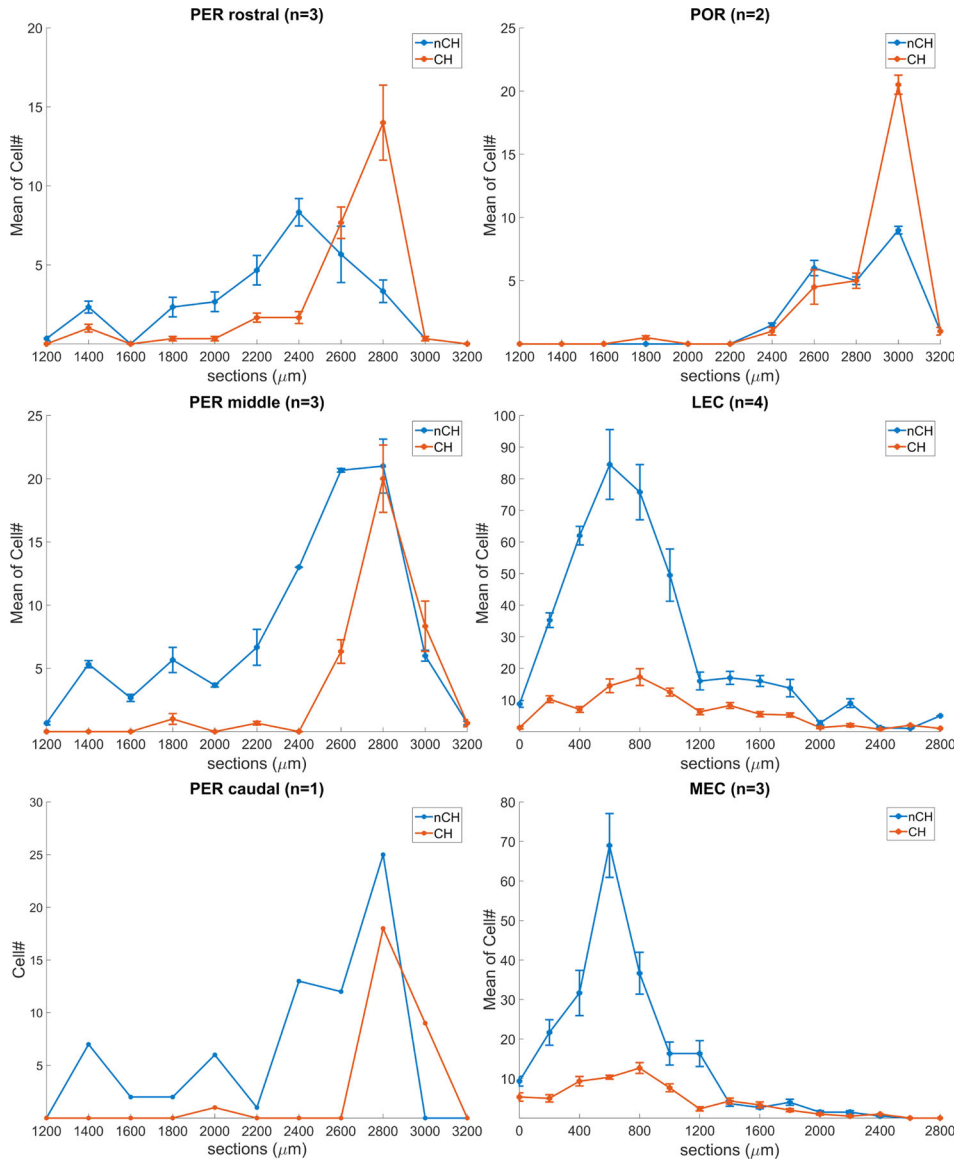

Figure 10. Graphical display of the normalized averaged cell numbers in the perirhinal (PER), postrhinal (POR), lateral entorhinal (LEC), and medial entorhinal (MEC) groups. Y axis: mean number of cholinergic (red) and noncholinergic (blue) neurons in the GP for PER and POR groups and in the MS/VDB, HDB, SI, and GP for LEC and MEC groups; X axis: distance in μm from the crossing of the anterior commissure (PER, POR cases). In LEC and MEC cases, 0 level corresponds to the appearance of the most rostral cholinergic neurons in the medial septum. Bars represent means ± SEM.

mapped the distribution of cholinergic and noncholinergic projection neurons to the PER in the entire BF and found that the BF projection neurons to the PER are present most densely in the caudal GP/SI and that the density of cholinergic projection neurons increases from rostral to caudal within the GP/SI. A few projection neurons to the PER were also observed in more rostral parts of the BF, including the SI, HDB, and VDB. The present study also revealed that about 26–48% of neurons that project to the PER are cholinergic, and there is a trend toward a higher cholinergic ratio in the rostral PER. The findings of our retrograde experiments are consistent with anterograde studies indicating that the GP, SI, and HDB give rise to labeling in the perirhinal cortex (Lamour et al., 1984; Saper, 1984; Luiten et al., 1985, 1987; Grove, 1988).

In previous studies that investigated BF projections to the cortex, the POR was not identified. The present study clarified that the topography of the BF projection (cholinergic and noncholinergic) to the POR is similar to that of the perirhinal cortex in that the caudal part of the GP/SI is the site that gives rise to the densest cholinergic and noncholinergic projections to the POR. However, the pattern of cholinergic and noncholinergic

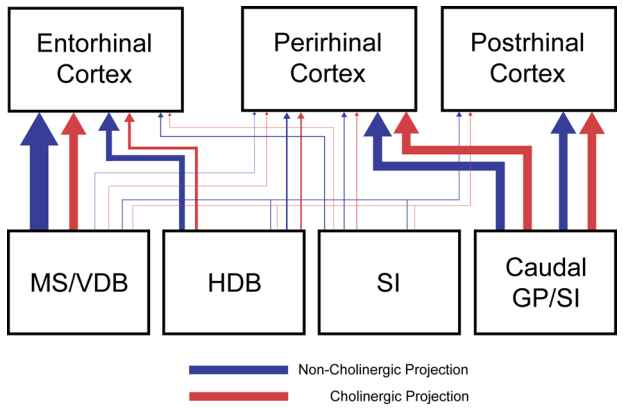

Figure 11. Summary of the topographic organization of BF projections to the perirhinal, postrhinal, and entorhinal cortex in rats. Red and blue lines indicate cholinergic and noncholinergic projections. Thickness of lines indicates the relative strength of projections. The perirhinal and postrhinal cortices receive cholinergic and noncholinergic projections mainly from the caudal basal forebrain (caudal GP and SI), whereas the entorhinal cortex receives projections mainly from the rostral basal forebrain (MS/VDB). Cholinergic neurons projecting to the perirhinal and postrhinal cortex comprise 26–48% of the total projection neurons (cholinergic and noncholinergic projection neurons) and 13–30% in the entorhinal cases. For abbreviations, see list.

projection neurons is slightly different from that of the perirhinal cases (Fig. 10). It remains to be investigated whether the same or different cholinergic cells project to these two cortical regions.

The present results for the EC are consistent with previous findings that the EC receives projections from the MS/VDB and HDB (Alonso and Kohler, 1984; Saper, 1984; Woolf et al., 1984; Manns et al., 2001). Furthermore, the present study provides new findings showing that projections to the LEC, compared with the MEC, extend further caudally in the BF. Our study also revealed that neurons that project to the MEC and LEC show distinct topography in the HDB (Fig. 7).

COMPARISON WITH THE BASAL FOREBRAIN PROJECTIONS TO OTHER CORTICAL REGIONS

Although the BF as a whole gives rise to projections to the entire cortical mantle, each cortical region receives topographically organized input from the BF (Bigl et al., 1982; Lamour et al., 1982; McKinney et al., 1983; Mesulam et al., 1983a,b; Price and Stern, 1983; Rye et al., 1984; Saper, 1984; Woolf et al., 1984; Amaral and Kurz, 1985; Luiten et al., 1987; Gaykema et al., 1990; Ghashghaei and Barbas, 2001; Bloem et al., 2014; Zaborszky et al., 2015a). For example, previous studies have shown that the temporal cortex, including the auditory, visual, and insular cortex, receives projections mainly from the caudal GP (Lamour et al., 1982; Price and Stern, 1983; Rye et al., 1984; Saper, 1984), which is similar to the pattern of BF projections to the perirhinal and postrhinal cortex we observed in the present study. In addition to a gross topography, it has been shown that interconnected cortical regions tend to receive projections from spatially overlapping pools of neurons in the BF (Zaborszky et al., 2015a). It is possible, although it remains to be examined, that the overlapping pool of neurons in the BF receives the same inputs and/or is interconnected via local collaterals and is thus capable of modulating the associated cortical areas in a coordinated fashion.

Supporting this idea, it has been shown that the PER and POR are reciprocally connected (Burwell and Amaral, 1998a; Agster and Burwell, 2009), and our study disclosed that the PER and POR receive projections from the same BF area. Interestingly, the lateral visual association cortex (area 18a) and the PER are interconnected (Shi and Cassel, 1997; Burwell and Amaral, 1998a), and BF projections to occipital area 18a (Carey and Rieck, 1987) and the PER (present study) seem to originate from a partially common BF area. Furthermore, the ventral auditory association cortex and the PER are interconnected (Shi and Cassel, 1997; Burwell and Amaral, 1998a; Paperna and Malach, 1991), and projections to these auditory areas (Price and Stern, 1983; Rye et al., 1984; Saper, 1984) and the PER (present study) originate from the partially common BF area. In addition, projections to S1/S2 cortical areas were shown to originate from the GP/internal capsule area (Baskerville et al., 1993), partially comparable to the location of BF cells projecting to the insular cortex (Zaborszky et al., 2015a) and PER (present study), and the S2 cortex projects via the insular cortex to the PER (Burwell and Amaral, 1998a; Shi and Cassel, 1998). It remains to be tested in future experiments whether indeed these pairs of cortical areas are jointly modulated by their BF input in specific cognitive operations.

The entorhinal cortex receives its cholinergic projection from the MS/VDB and HDB areas. Interestingly, the medial visual association cortex (18b) and the MEC receive BF projections from a partially common BF region (Rieck and Carey, 1984), and the MEC projects to the medial visual area (Agster and Burwell, 2009). The retrosplenial cortex (RS) also receives its BF projection from the MS/VDB/HDB area (Saper, 1984; Gyengesi et al., 2013), and the MEC projects to the retrosplenial cortex (Insausti et al., 1997; Agster and Burwell, 2009). Furthermore, the medial visual cortex and the RS are reciprocally connected (Vogt and Miller, 1983).

The hippocampus receives BF projections mainly from the MS/VDB (McKinney et al., 1983; Rye et al.,

1984; Saper, 1984; Woolf et al., 1984; Amaral and Kurz, 1985; Gaykema et al., 1990). The topographic pattern of the BF projection to the hippocampus is similar to that to the entorhinal cortex, as we observed in the present study, and these structures are interconnected (Witter et al., 2000). Although the PER/POR and entorhinal cortex are interconnected, the BF projections to these areas originate from very different BF regions. This indicates that the notion that interconnected cortical areas receive projections from overlapping pool of BF neurons may not apply for every cortical region.

The perirhinal and postrhinal cortex receive convergent inputs from several association cortices (Suzuki and Amaral, 1994; Burwell and Amaral, 1998a) and provide cortical input to the entorhinal cortex, which in turn sends major cortical input to the hippocampus (Naber et al., 1997; Burwell and Amaral, 1998a,b; Witter et al., 2000). The cortico-hippocampal pathway consists of two parallel but interacting pathways (Witter et al., 2000) so that the perirhinal cortex sends projections mainly to the LEC, whereas the postrhinal cortex projects mainly to the MEC (Naber et al., 1997; Burwell and Amaral, 1998b). The perirhinal cortex and the LEC are important for processing object or nonspatial information (Hargreaves et al., 2005; Winters and Bussey, 2005a,b; Deshmukh and Knierim, 2011), whereas the postrhinal cortex and MEC are important for processing object-place, contextual information (Furtak et al., 2012) and spatial information (Hargreaves et al., 2005; Moser et al., 2008), respectively. Although PER and POR projection neurons are located in the same BF area (i.e., the GP), there are subtle differences in their projection pattern (Fig. 10).

Previous studies have shown that disruption of cholinergic transmission in the perirhinal cortex impairs object recognition (Tang et al., 1997; Winters and Bussey, 2005b). The observation that the perirhinal and lateral visual association cortex receive their input from a partially common BF space (caudal GP/SI) is compatible with the suggestion that the visual and perirhinal cortex is jointly modulated through BF cholinergic input to support specific cognitive function. Future functional studies are needed to establish the significance of the observation that the medial visual association area, the retrosplenial cortex, and the entorhinal cortex receive their cholinergic input from the partially common BF region in the septum.

Cholinergic, GABAergic, and glutamatergic projections

BF projection neurons comprise cholinergic, GABAergic, and glutamatergic neurons (Gritti et al., 1997; Manns et al., 2001; Hur and Zaborszky, 2005; Henny and Jones, 2008). In the present study, cholinergic projection neurons to the perirhinal/postrhinal and entorhinal cortex were found to make up approximately 26–48% and 13–30% of the total number of projection neurons, respectively.

GABAergic BF neurons project to the entorhinal cortex (Manns et al., 2001), and the small proportion of cholinergic projection neurons to the entorhinal cortex suggests that noncholinergic, possibly GABAergic modulation becomes important. It was recently shown that cortically projecting GABAergic neurons containing parvalbumin, which send projections to cortical parvalbumin interneurons, are important for enhancing cortical gamma band oscillations (Kim et al., 2015). Cholinergic neurons excite cortically projecting GABAergic neurons via their collaterals in the BF (Yang et al., 2014), and the differential contribution of cholinergic projections to the perirhinal and entorhinal cortex suggests that GABAergic and cholinergic modulation of these cortical areas is under complex regulation.

In a study investigating the BF projections to the entorhinal cortex (Manns et al., 2001), it was suggested that a substantial fraction of the projection to this cortical area is glutamatergic, based on the presence of phosphate-activated glutaminase (PAG). However, PAG is not a specific marker for glutamatergic neurons. Using a specific marker for glutamatergic neurons, it was shown that only 5% of BF projections are directed to the prefrontal or somatosensory cortex (Hur and Zaborszky, 2005). Future studies will elucidate the contribution of BF glutamatergic neurons projecting to the entorhinal cortex.

ACKNOWLEDGMENTS

The authors thank Peter Gombkoto, Ph.D., for preparing Figure 10.

CONFLICT OF INTEREST STATEMENT

The authors declare they have no conflicts of interest

ROLE OF AUTHORS

Both authors had full access to all the data in the study and take full responsibility for the integrity of the data and the accuracy of the data analysis. H.K. and L.Z. conceived and designed the study, performed data analysis with interpretation, and drafted manuscript. H.K. performed all the experiments, and did the histology and mapping of the sections.

LITERATURE CITED

Agster KL, Burwell RD. 2009. Cortical efferents of the perirhinal, postrhinal, and entorhinal cortices of the rat. Hippocampus 19:1159–1186

Alonso A, Kohler C. 1984. A study of the reciprocal connections between the septum and the entorhinal area using anterograde and retrograde axonal transport methods in the rat brain. J Comp Neurol 225:327–343.

Amaral DG, Kurz J. 1985. An analysis of the origins of the cholinergic and noncholinergic septal projections to the hippocampal formation of the rat. J Comp Neurol 240: 37–59.

Baskerville KA, Chang HT, Herron P. 1993. Topography of cholinergic afferents from the nucleus basalis of Meynert to representational areas of sensorimotor cortices in the rat. J Comp Neurol 335:552–562.

Bigl V, Woolf NJ, Butcher LL. 1982. Cholinergic projections from the basal forebrain to frontal, parietal, temporal, occipital, and cingulate cortices: a combined fluorescent tracer and acetylcholinesterase analysis. Brain Res Bull 8:727–749.

Bloem B, Schoppink L, Rotaru DC, Faiz A, Hendriks P, Mansvelder HD, van de Berg WD, Wouterlood FG. 2014. Topographic mapping between basal forebrain cholinergic neurons and the medial prefrontal cortex in mice. J Neurosci 34:16234–16246.

Burwell RD. 2001. Borders and cytoarchitecture of the perirhinal and postrhinal cortices in the rat. J Comp Neurol 437:17–41.

Burwell RD, Amaral DG. 1998a. Cortical afferents of the perirhinal, postrhinal, and entorhinal cortices of the rat. J Comp Neurol 398:179–205.

Burwell RD, Amaral DG. 1998b. Perirhinal and postrhinal cortices of the rat: interconnectivity and connections with the entorhinal cortex. J Comp Neurol 391:293–321.

Buzsaki G, Bickford RG, Ponomareff G, Thal LJ, Mandel R, Gage FH. 1988. Nucleus basalis and thalamic control of neocortical activity in the freely moving rat. J Neurosci 8: 4007–4026.

Carey RG, Rieck RW. 1987. Topographic projections to the visual cortex from the basal forebrain in the rat. Brain Res 424:205–215.

Deshmukh SS, Knierim JJ. 2011. Representation of non-spatial and spatial information in the lateral entorhinal cortex. Front Behav Neurosci 5:69.

Detari L, Rasmusson DD, Semba K. 1999. The role of basal forebrain neurons in tonic and phasic activation of the cerebral cortex. Prog Neurobiol 58:249–277.

Dringenberg HC, Vanderwolf CH. 1998. Involvement of direct and indirect pathways in electrocorticographic activation. Neurosci Biobehav Rev 22:243–257.

Duque A, Balatoni B, Detari L, Zaborszky L. 2000. EEG correlation of the discharge properties of identified neurons in the basal forebrain. J Neurophysiol 84:1627–1635.

Everitt BJ, Robbins TW. 1997. Central cholinergic systems and cognition. Annu Rev Psychol 48:649–684.

Fuller PM, Sherman D, Pedersen NP, Saper CB, Lu J. 2011. Reassessment of the structural basis of the ascending arousal system. J Comp Neurol 519:933–956.

Furtak SC, Wei SM, Agster KL, Burwell RD. 2007. Functional neuroanatomy of the parahippocampal region in the rat: the perirhinal and postrhinal cortices. Hippocampus 17: 709–722.

Furtak SC, Ahmed OJ, Burwell RD. 2012. Single neuron activity and theta modulation in postrhinal cortex during visual object discrimination. Neuron 76:976–988.

Gaykema RP, Luiten PG, Nyakas C, Traber J. 1990. Cortical projection patterns of the medial septum-diagonal band complex. J Comp Neurol 293:103–124.

Ghashghaei HT, Barbas H. 2001. Neural interaction between the basal forebrain and functionally distinct prefrontal cortices in the rhesus monkey. Neuroscience 103:593–614.

Gritti I, Mainville L, Mancia M, Jones BE. 1997. GABAergic and other noncholinergic basal forebrain neurons, together with cholinergic neurons, project to the mesocortex and isocortex in the rat. J Comp Neurol 383:163–177.

Grove EA. 1988. Efferent connections of the substantia innominata in the rat. J Comp Neurol 277:347–364.

Gyengesi E, Andrews ZB, Paxinos G, Zaborszky L. 2013. Distribution of secretagogin-containing neurons in the basal forebrain of mice, with special reference to the cholinergic corticopetal system. Brain Res Bull 94:1–8.

Hargreaves EL, Rao G, Lee I, Knierim JJ. 2005. Major dissociation between medial and lateral entorhinal input to dorsal hippocampus. Science 308:1792–1794.

Henny P, Jones BE. 2008. Projections from basal forebrain to prefrontal cortex comprise cholinergic, GABAergic and glutamatergic inputs to pyramidal cells or interneurons. Eur J Neurosci 27:654–670.

Hur EE, Zaborszky L. 2005. Vglut2 afferents to the medial prefrontal and primary somatosensory cortices: a combined retrograde tracing in situ hybridization study. J Comp Neurol 483:351–373.

Insausti R, Herrero MT, Witter MP. 1997. Entorhinal cortex of the rat: cytoarchitectonic subdivisions and the origin and distribution of cortical efferents. Hippocampus 7:146–183.

Jones BE. 2004. Activity, modulation and role of basal forebrain cholinergic neurons innervating the cerebral cortex. Prog Brain Res 145:157–169.

Kim T, Thankachan S, McKenna JT, McNally JM, Yang C, Choi JH, Chen L, Kocsis B, Deisseroth K, Strecker RE, Basheer R, Brown RE, McCarley RW. 2015. Cortically projecting basal forebrain parvalbumin neurons regulate cortical gamma band oscillations. Proc Natl Acad Sci U S A 112: 3535–3540.

Lamour Y, Dutar P, Jobert A. 1982. Topographic organization of basal forebrain neurons projecting to the rat cerebral cortex. Neurosci Lett 34:117–122.

Lamour Y, Dutar P, Jobert A. 1984. Cortical projections of the nucleus of the diagonal band of Broca and of the substantia innominata in the rat: an anatomical study using the anterograde transport of a conjugate of wheat germ agglutinin and horseradish peroxidase. Neuroscience 12: 395–408.

Letzkus JJ, Wolff SB, Meyer EM, Tovote P, Courtin J, Herry C, Luthi A. 2011. A disinhibitory microcircuit for associative fear learning in the auditory cortex. Nature 480:331–335.

Lin SC, Nicolelis MA. 2008. Neuronal ensemble bursting in the basal forebrain encodes salience irrespective of valence. Neuron 59:138–149.

Luiten PG, Spencer DG Jr, Traber J, Gaykema RP. 1985. The pattern of cortical projections from the intermediate parts of the magnocellular nucleus basalis in the rat demonstrated by tracing with *Phaseolus vulgaris*-leucoagglutinin. Neurosci Lett 57:137–142.

Luiten PG, Gaykema RP, Traber J, Spencer DG Jr. 1987. Cortical projection patterns of magnocellular basal nucleus subdivisions as revealed by anterogradely transported *Phaseolus vulgaris* leucoagglutinin. Brain Res 413:229–250.

Manns ID, Mainville L, Jones BE. 2001. Evidence for glutamate, in addition to acetylcholine and GABA, neurotransmitter synthesis in basal forebrain neurons projecting to the entorhinal cortex. Neuroscience 107:249–263.

McKinney M, Coyle JT, Hedreen JC. 1983. Topographic analysis of the innervation of the rat neocortex and hippocampus by the basal forebrain cholinergic system. J Comp Neurol 217:103–121.

Mesulam MM, Mufson EJ, Wainer BH, Levey AI. 1983a. Central cholinergic pathways in the rat: an overview based on an alternative nomenclature (Ch1-Ch6). Neuroscience 10:1185–1201.

Mesulam MM, Mufson EJ, Levey AI, Wainer BH. 1983b. Cholinergic innervation of cortex by the basal forebrain: cytochemistry and cortical connections of the septal area, diagonal band nuclei, nucleus basalis (substantia innominata), and hypothalamus in the rhesus monkey. J Comp Neurol 214:170–197.

Metherate R, Cox CL, Ashe JH. 1992. Cellular bases of neocortical activation: modulation of neural oscillations by the nucleus basalis and endogenous acetylcholine. J Neurosci 12:4701–4711.

Moser EI, Kropff E, Moser MB. 2008. Place cells, grid cells, and the brain's spatial representation system. Annu Rev Neurosci 31:69–89.

Muir JL, Page KJ, Sirinathsinghji DJ, Robbins TW, Everitt BJ. 1993. Excitotoxic lesions of basal forebrain cholinergic neurons: effects on learning, memory and attention. Behav Brain Res 57:123–131.

Naber PA, Caballero-Bleda M, Jorritsma-Byham B, Witter MP. 1997. Parallel input to the hippocampal memory system through peri- and postrhinal cortices. Neuroreport 8: 2617–2621.

Paperna T, Malach R. 1991. Patterns of sensory intermodality relationships in the cerebral cortex of the rat. J Comp Neurol 308:432–456.

Paxinos G, Watson C. 2005. The rat brain in stereotaxic coordinates, 5th ed. Cambridge, MA: Elsevier Academic Press.

Pinto L, Goard MJ, Estandian D, Xu M, Kwan AC, Lee SH, Harrison TC, Feng G, Dan Y. 2013. Fast modulation of visual perception by basal forebrain cholinergic neurons. Nat Neurosci 16:1857–1863.

Price JL, Stern R. 1983. Individual cells in the nucleus basalis–diagonal band complex have restricted axonal projections to the cerebral cortex in the rat. Brain Res 269:352–356.

Rieck R, Carey RG. 1984. Evidence for a laminar organization of basal forebrain afferents to the visual cortex. Brain Res 297:374–380.

Rye DB, Wainer BH, Mesulam MM, Mufson EJ, Saper CB. 1984. Cortical projections arising from the basal forebrain: a study of cholinergic and noncholinergic components employing combined retrograde tracing and immunohistochemical localization of choline acetyltransferase. Neuroscience 13:627–643.

Saper CB. 1984. Organization of cerebral cortical afferent systems in the rat. II. Magnocellular basal nucleus. J Comp Neurol 222:313–342.

Shi CJ, Cassell MD. 1997. Cortical, thalamic, and amygdaloid projections of rat temporal cortex. J Comp Neurol 382: 153–175.

Shi CJ, Cassell MD. 1998. Cascade projections from somatosensory cortex to the rat basolateral amygdala via the parietal insular cortex. J Comp Neurol 399:469–491.

Suzuki WA, Amaral DG. 1994. Perirhinal and parahippocampal cortices of the macaque monkey: cortical afferents. J Comp Neurol 350:497–533.

Tang Y, Mishkin M, Aigner TG. 1997. Effects of muscarinic blockade in perirhinal cortex during visual recognition. Proc Natl Acad Sci U S A 94:12667–12669.

Unal CT, Golowasch JP, Zaborszky L. 2012. Adult mouse basal forebrain harbors two distinct cholinergic populations defined by their electrophysiology. Front Behav Neurosci 6: 1–14.

Unal CT, Pare D, Zaborszky L. 2015. Impact of basal forebrain cholinergic inputs on basolateral amygdala neurons. J Neurosci 35:853–863.

Vogt BA, Miller MW. 1983. Cortical connections between rat cingulate cortex and visual, motor, and postsubicular cortices. J Comp Neurol 216:192–210.

Winters BD, Bussey TJ. 2005a. Transient inactivation of perirhinal cortex disrupts encoding, retrieval, and consolidation of object recognition memory. J Neurosci 25:52–61.

Winters BD, Bussey TJ. 2005b. Removal of cholinergic input to perirhinal cortex disrupts object recognition but not spatial working memory in the rat. Eur J Neurosci 21:2263–2270.

Witter MP, Wouterlood FG, Naber PA, Van Haeften T. 2000. Anatomical organization of the parahippocampal-hippocampal network. Ann N Y Acad Sci 911:1–24.

Woolf NJ, Eckenstein F, Butcher LL. 1984. Cholinergic systems in the rat brain: I. projections to the limbic telencephalon. Brain Res Bull 13:751–784.

Yang C, McKenna JT, Zant JC, Winston S, Basheer R, Brown RE. 2014. Cholinergic neurons excite cortically projecting basal forebrain GABAergic neurons. J Neurosci 34:2832–2844.

Zaborszky L, Csordas A, Mosca K, Kim J, Gielow MR, Vadasz C, Nadasdy Z. 2015a. Neurons in the basal forebrain project to the cortex in a complex topographic organization that reflects corticocortical connectivity patterns: an experimental study based on retrograde tracing and 3D reconstruction. Cereb Cortex 25:118–137.

Zaborszky L, Duque A, Gielow M, Gombkoto P, Nadasdy Z, Somogyi J. 2015b. Organization of the basal forebrain cholinergic projection system: specific or diffuse? In Paxinos G, ed. The rat nervous system, 4th ed. Amsterdam: Elsevier. pp 491–507.

Zaborszky L, Amunts K, Palomero-Gallagher N, Zilles K. 2015c. Basal forebrain anatomical systems in MRI space. In Toga A, ed. Brain mapping: an encyclopedic reference. Amsterdam: Elsevier. pp 395–409.